

A design study of ILC positron source by electron driven scheme

M. Kuriki*, Y. Seimiya, T. Takahashi, HU/AdSM, Higashihiroshima
T. Okugi, M. Satoh, J. Urakawa, Accelerator Lab., KEK, Tsukuba
T. Omori, IPNS, KEK, Tsukuba
S. Kashiwagi, RCEPS, Tohoku U., Sendai

Abstract

ILC (International Linear Collider) is an e⁺ and e⁻ collider based on linear accelerators. ILC is the most desirable future project of high energy physics for detail study of Higgs sector and hunting new particles such as SUSY particles. The current baseline design of ILC positron source is based on gamma ray conversion from undulator radiation. This scheme is attractive from physics point of view because polarized positron is generated. On the other hand, this approach is totally new and it is very difficult to demonstrate the system prior to the construction because it requires more than 100 GeV beam as the driver. From a project management point of view, a technical backup based on a well established technology is desirable. A conventional positron generation (e⁻ driven) for ILC can be the solution. In this method, the technology is well established, but the heat load on the production target can be the biggest issue. We present a result of a simulation study of the e⁻ driven ILC positron source. By employing 6 GeV e⁻ beam as the driver, an enough amount of e⁺ can be generated in the acceptance defined by DR (Damping Ring). The target heat load is kept below the practical damage limit established by SLC.

INTRODUCTION

International Linear Collider (ILC) is a future project of high energy physics. It is an electron and positron linear collider based on the Super-conducting accelerator with its CME (Center of Mass Energy) 500 GeV in the first phase and 1 TeV in the second phase. The design luminosity at 500 GeV is $2.0 \times 10^{34} \text{ cm}^{-2} \text{ s}^{-1}$. Technical Design Report of ILC has been published in 2013[1]. The Japanese candidate site has been selected as Kitakami Mt. area, Iwate prefecture and the technical detail design including site specific parts (e.g. access tunnel layout, etc.) is progressed. In ILC, the positron is generated by undulator method. In this method, the driver electron beam generates high energy gamma ray by passing through undulator. The gamma ray is converted to positron by pair-creation process with Ti-alloy target. For the efficient conversion, the gamma ray energy is at least more than 10 MeV which requires 130 GeV drive electron beam energy with 10 mm undulator period. An electron linac dedicated to the driver is not realistic and the electron beam for collision is shared with the undulator. This is a totally new approach as positron source and a system demonstration prior to the real construction is

desirable, but it is therefore practically difficult. By considering the risk control of a project, it is not an ideal situation. If we have a technical backup for the ILC positron source, it reduces unknown technical risks related to this totally new approach.

Conventional positron generation for linear colliders has been proposed and it is also considered for ILC[2]. In this proposal, several GeV electron beam impinges on a heavy metal target (typically W-Re) and positron is generated by Bremsstrahlung. Possible target destruction is the biggest issue in this case. According to SLC experience, Peak Energy Deposition Density (PEDD) given by incident electron beam has to be less than 35 J/g[3][4][5]. Our goal is establishing the positron injector design to achieve enough amount of positron for ILC keeping PEDD less than the limit.

ILC ELECTRON DRIVEN POSITRON SOURCE

In this section, ILC electron driven Positron source is described. The layout is shown in Fig. 1. It consists from electron linac, conversion target, AMD (Adiabatic Matching Device) for transverse momentum suppression, positron injector with focusing solenoid for positron capturing, chicane to remove electrons energy deviated positrons, positron booster up to 5 GeV, and ECS (Energy Compressor Section). Our goal is providing an enough amount of positron to DR whose dynamic aperture is $\gamma A_x + \gamma A_y < 0.07$ in the transverse space and $z < \pm 35 \text{ mm}$ and $\delta < \pm 0.0075$ in longitudinal space, where A_x and A_y are action value, δ is relative energy deviation. As a design criteria, 50% margin on the number of positron in DR is required. Number of positron in each bunch at IP (Interaction Point) should be 2.0×10^{10} , then 3.0×10^{10} positrons in DR acceptance is required.

PEDD gives a practical limit on the positron intensity on the production target. It should be less than 35 J/g according to SLC experience[3][4][5]. In the ILC positron generation, number of required positron per second is 50 times larger than that of SLC and the target might be easily broken. To compensate PEDD, 63 ms out of 199 ms which is ILC pulse interval, is used for positron generation. In the 63 ms, 20 RF pulses are fired in 300 Hz. For each RF pulses, 132 bunches are contained in a form of a triplet where each mini-trains contain 44 bunches with 6.15 ns spacing and the mini-train interval is 100 ns[2]. Duration and average beam current of one triplet is about 1 μs and 0.63 A and it is feasible to employ Normal Con-

* mkuriki@hiroshima-u.ac.jp

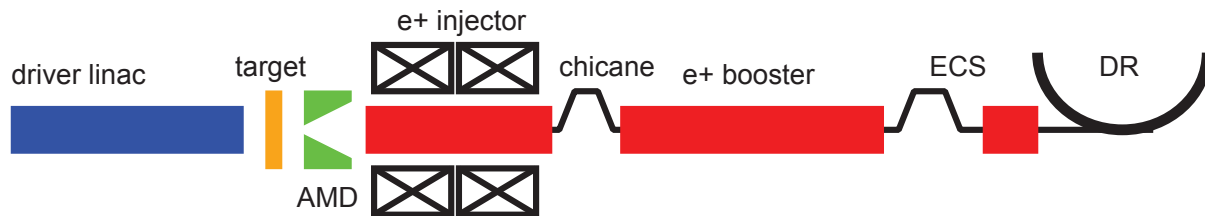


Figure 1: Layout of the ILC electron driven positron source which consists from electron linac, target, AMD, positron injector, positron booster, and ECS.

ducting (NC) RF system for the acceleration. By considering positron capture performance and cost effectiveness, L-band and S-band NC accelerators are employed.

The beam energy and bunch intensity of the driver linac is typically 6 GeV and 2.0×10^{10} , respectively. The target is 14 mm thick rotating target made from W-Re alloy which has a good conversion efficiency. The rotation could be up to 5 m/s tangential speed to suppress PEDD below 35 J/g and spread out the heat load. AMD induces a strong magnetic field along the beam axis. The peak field is typically 5 Tesla and the field is smoothly connected to the solenoid field at the positron injector, 0.5 Tesla. AMD magnetic field is generated by Flux concentrator which should be similar to that designed for Super-KEKB factory at KEK, Japan[6].

In this scheme, 132 bunches in a triplet impinge on a same spot on the target. PEDD is not exceeded 35 J/g with this one triplet. Before bunches in the next triplet arrive at the target, it takes 3.3ms and the target moves by 16.5mm. The target shift is more than 4σ by assuming 4 mm rms spot size on the electron beam. According to this consideration, PEDD is kept at that by one triplet even we continue injection over 63 ms.

The positron injector linac is composed from L-band NC accelerators with 0.5 Tesla focusing solenoid field. The energy is up to 250 MeV. After the injector linac, a chicane section is inserted to remove electrons and positrons with a large energy deviation. Figure 2 shows beta and dispersion functions of the chicane section.

The positron booster is composed from L-band and S-band NC accelerators as a result of optimization which will be mentioned in the next section. The positron is accelerated by the booster up to 5 GeV. Figure 3 shows the lattice configuration and optical design of the booster. After the booster, ECS (Energy Compressor Section) is placed. DR acceptance in the longitudinal space is 70 mm in z and 1.5% in δ , respectively. The z acceptance is too wide comparing to the δ acceptance, because the energy spread by RF curvature assuming L-band or S-band acceleration with 70 mm bunch length is much larger than 1.5%. Phase-space rotation by ECS in the longitudinal space improves the effective area of the DR acceptance. In other words, ECS optimizes the capture efficiency. Figure 4 shows allowed energy spread before the booster as a function of the bunch length. In this calculation, the energy spread δ at the end of the positron injection and that by the RF curvature in

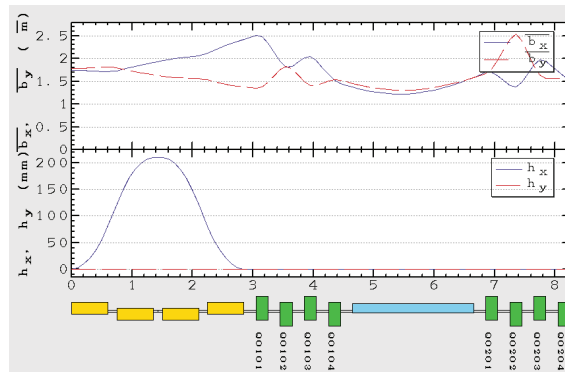


Figure 2: Beta function (upper) and dispersion function (lower) in the chicane section. Horizontal axis shows distance from the top of the chicane section. The lower picture shows magnet lattice.

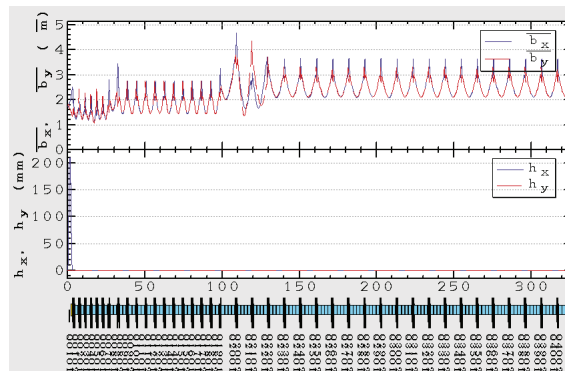


Figure 3: Beta function (upper) and dispersion function (lower) in the chicane and the booster. Horizontal axis shows distance from the top of the chicane section. The lower picture shows magnet lattice.

the booster linac are linearly added. Both axes are in full width. Areas below the solid and dashed lines corresponds to the allowed regions by S-band and L-band booster, respectively. For example, if the captured positron bunch in the injector has 200 MeV in energy and 10 mm in z , it can be accepted by DR with the ECS phase space rotation. It is not possible without ECS, because 200 MeV energy spread is already more than 1.5% of 5 GeV. R_{56} of ECS is 1 m or less. From this point of view, both S-band and L-band are

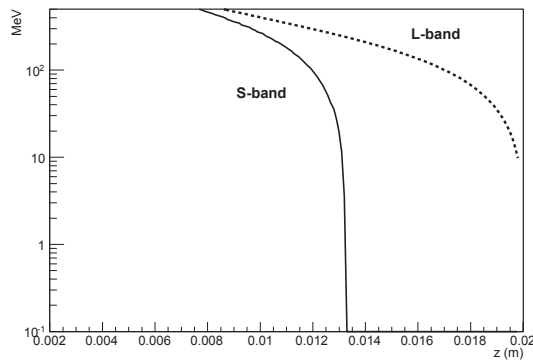


Figure 4: Allowed region of energy spread and bunch length at the injector with ECS is shown. Below each lines (solid for S-band and dashed for L-band) are allowed.

Table 1: A typical parameter set. Aperture is given in radius.

Parameter	Value	Unit
Drive Beam energy	6.0	GeV
Beam size	4.0	mm (RMS)
AMD peak field	5.0	Tesla
RF Gradient	25	MV/m
Injector L-band RF aperture	20	mm
Booster L-band RF aperture	17	mm
Booster S-band RF aperture	10	mm
Solenoid	0.5	Tesla

acceptable for the booster, however, the first half should be L-band and the last half can be S-band by considering the transverse aperture discussed in the next section.

POSITRON CAPTURE SIMULATION

In this section, results of the tracking simulations are presented. Positron generated by the electron injection with W-Re target is simulated by GEANT4 and the data used in this simulation are almost identical to those in Ref.[2]. The data are imported to GPT[7] to perform the tracking simulation in the positron injector. After the chicane, including the booster up to 5 GeV and ECS, the simulation is performed by SAD[8]. As a reference, the simulations are performed with parameters as shown in table 1.

Positron generated in the target is captured by AMD followed by injector linac with solenoid focusing. At the end of the injector, the beam energy is 250 MeV, but the energy spread is large. After the injector, there is a chicane section. There are two roles for the chicane. One is removing electrons from the beam. From the EM shower, not only positrons, but also electrons are obtained. The electron has opposite electrical charge and captured by the injector on the other RF phase than that for positron. Due to this reversed phase, the electron gives the same beam

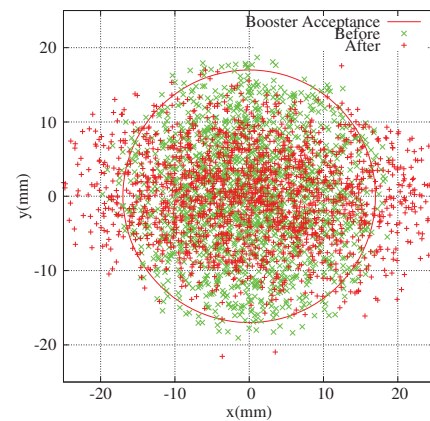


Figure 5: Particle distribution in transverse space at the end of the injector where the beam energy is 250 MeV. The diagonal and right cross symbols show particles before and after chicane.

loading as that by the positrons. Then, electrons have to be removed as early as possible to compensate the beam loading effect. Another role of the chicane is removing positron with a large energy deviation. Such positron will be lost anyway before DR injection, but the beam loss after acceleration causes high radiation and activation. Then, such positron should be removed as early as possible. By considering these reasons, the chicane at the lower energy is better. On the other hand, the capture efficiency for the positron will be affected if the chicane is placed at the lower energy region. The place of the chicane is determined by compromising between these two facts. In this simulation, the chicane is placed after the injector where the beam energy is 250 MeV. It is not fully optimized, but an enough capture efficiency is obtained with this configuration as we will see. Quantifying the beam loading effect and the beam loss will be studied as next issues. Figure 5 and 6 show the particle distributions in the transverse space (xy) and longitudinal space ($z - \delta$), respectively. In both figures, particles before and after the chicane sections are plotted with diagonal and right cross symbols. In Fig. 5, the accelerator aperture is shown by the red circle for reference. The chicane increases the horizontal beam size, but it can be focused again after the chicane. Efficiency loss by inserting the chicane is not significant. In Fig. 6, z position shift for lower energy particles is recognized. This shift is due to the dispersion. By comparing capture efficiency with and without chicane, it is slightly improved with the chicane. For each cases, other parameters like RF phase are optimized and the exact reason is not well understood. One possibility is that the $x - \delta$ correlation made with this chicane compensates energy spread after the booster. Less energy spread might improved the capture efficiency, but the detail should be studied.

The longitudinal phase space distribution after ECS is shown in Fig. 7. The particle distribution is rotated by ECS as recognized. The particle distribution after ECS is exam-

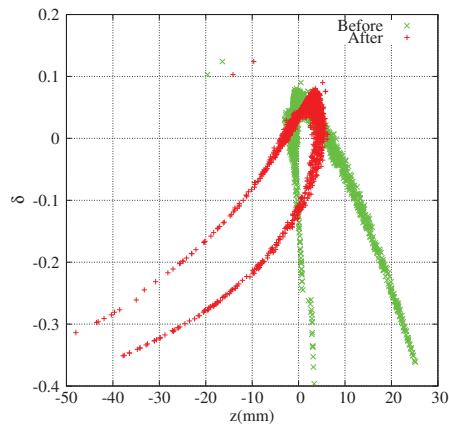


Figure 6: Particle distribution in longitudinal space at the end of the injector where the beam energy is 250 MeV. The diagonal and right cross symbols show particles before and after chicane.

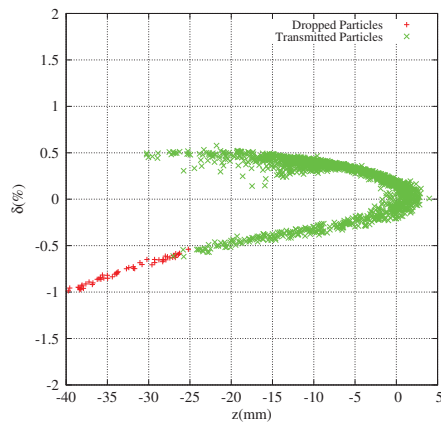


Figure 7: Particle distribution in longitudinal space after ECS.

ined with DR acceptance and number of accepted positron is counted as yield which is defined as ratio of the accepted positron with number of electron.

Fig. 8 shows the yield as a function of AMD aperture for 5 Tesla (solid line), 7 Tesla (dashed line), and 9 Tesla (dotted line) peak field. The target end is located at 5 mm upstream from where AMD field is peaked. Larger aperture gives better yield, but aperture more than 8 mm does not give any big gain. For the peak field, 5 Tesla shows the best among them. According to this results, 5 Tesla peak field with 8 mm aperture is an optimum.

Fig. 9 shows the yield as a function of aperture of accelerating structure in radius at the beginning of the booster linac. Larger aperture gives better yield, but the yield is already saturated at 16 mm. The beam size is reduced with acceleration by adiabatic damping effect and this aperture corresponds to L-band structure which is used in the first half of the booster.

By considering cost effectiveness, S-band accelerator is better than L-band. Up to now, the simulation is performed with L-band structure. Here, we examined the yield by re-

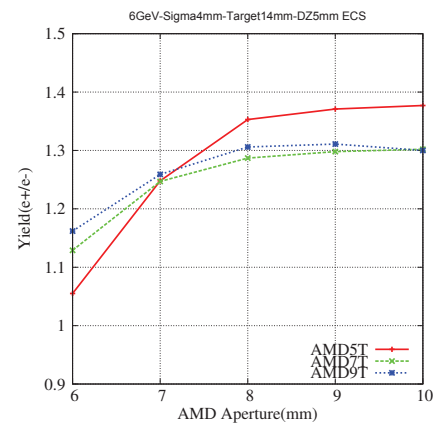


Figure 8: Yield as a function of AMD aperture for 5, 7, and 9 Tesla peak field. 5 Tesla peak field gives the best yield.

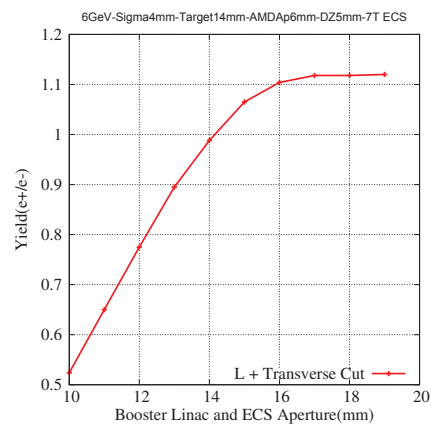


Figure 9: Yield as a function of aperture of accelerating structure.

placing the L-band with the S-band. Aperture of the S-band structure is assumed to be 10mm in radius. The result is shown in Fig. 10. There are totally 40 cells of the lattice in the booster linac. In this figure, the yield is estimated when the L-band structures after the cell are replaced with the S-band. From this plot, the yield defined as number of captured positrons and injected electrons is decreased when we replace large number of cells with S-band. However, as we mention later, the yield 1.28 gives an enough amount of positron in the DR acceptance. 26 and later cells can be replaced with the S-band.

Finally, the drive beam and target configuration is optimized according to the yield calculated by the tracking simulation. By changing the drive beam energy, target thickness, and the spot size, PEDD and energy deposition per bunch are varied. To compare performances with different configurations, the bunch intensity is varied giving the same number of positron in the DR acceptance, $3.0 \times 10^{10}/bunch$, i.e. the condition is normalized by the number of captured positron. In Fig. 11, various target and beam configurations are plotted in PEDD (horizontal axis) and Energy deposition per bunch (vertical axis). The numbers associated to each points show the drive beam energy,

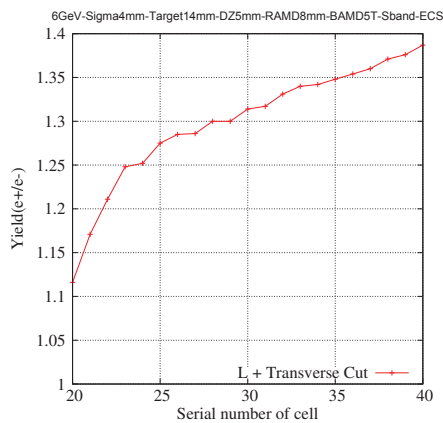


Figure 10: Yield as a function of cell number where L-band ends.

target thickness, and the beam spot size in rms. As a practical limit, PEDD should be less than 35 J/g to prevent any target destruction and some conditions are excluded. For the energy deposition per bunch, there is no clear threshold, however, the lower is better from technical point of view. Among these configurations, 6 GeV driver beam energy, 14 mm target thickness, and 4 mm rms spot size is the best.

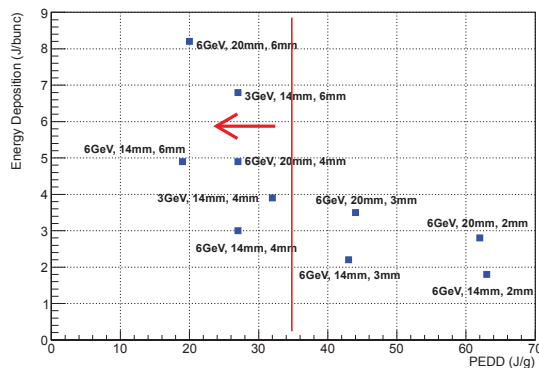


Figure 11: PEDD (J/g) and Energy deposition per bunch with various configurations. 6 GeV drive beam energy, 14 mm target thickness, and 4 mm rms spot size is the best.

SUMMARY AND CONCLUSION

We perform a start-to-end simulation for the electron driven ILC positron source. According to the simulation, 3.0×10^{10} positron per bunch is obtained with PEDD 27 J/g which is below the practical limit by SLC, 35 J/g. The spot size on the target is 4 mm (RMS) and the bunch intensity of the driver linac is 2.3×10^{10} electrons per bunch. AMD peak field is 5 Tesla with 8 mm aperture. The injector linac is L-band with 0.5 Tesla solenoid-focusing. The booster linac is a hybrid of L-band and S-band structures. ECS is important for better acceptance. The beam chicane

to remove electrons and positrons with a large energy deviation has a limited impact on the capture efficiency.

ILC is now in a stage of the technical detail design which should be completed in three years. Based on the positron source design described in this report, we have to establish a technical design to synchronize to the global ILC schedule. Among various issues which should be studied before the technical design, the effect of beam loading, especially in the positron injector should be carefully studied, because the beam loading in the positron injector can be very heavy by electrons. The electrons give the same beam loading since they are captured in the opposite phase of RF. After confirming various issues, we can start the technical design of the electron driven positron source for ILC.

ACKNOWLEDGEMENT

This work is partly supported by Grant-in-Aid for Scientific Research (C 26400293).

REFERENCES

- [1] ILC TDR, ISBN 978-3-935702-74-4 (2013).
- [2] T. Omori et al., NIMA**672**(2012)52-56.
- [3] T. Kamitani and L.Rinolfi, CLIC-NOTE-465 CERN-OPEN-2001-025.
- [4] S.Ecklund, SLAC-CN128(1981).
- [5] NLC Collaboration, SLAC-R-571, 2001.
- [6] L. Zang et al., Proc. of IPAC(2012)TUPPD032.
- [7] Pulsar Physics Home page, "<http://www.pulsar.nl/gpt/index.html>".
- [8] SAD Home page, "<http://acc-physics.kek.jp/SAD/>".